Inhibit the formation of toxic methylphenolic by-products in photo-decomposition of formaldehyde–toluene/xylene mixtures by Pd cocatalyst on TiO2

Qiqi Wu [a,b], Jiani Ye [a], Wei Qiao [a,**], Yongwang Li [b, c], J.W. (Hans) Niemantsverdriet [b,d], Emma Richards [e], Feng Pan [f,**], Ren Su [a,b,*]

[a] Soochow Institute for Energy and Materials InnovationS (SIEMIS), Key Laboratory of Advanced Carbon Materials and Wearable Energy Technologies of Jiangsu Province, Soochow University, Suzhou, 215006, China
[b] SynCat@Beijing, Synfuels China Technology Co. Ltd., Leyuan South Street II, No.1, Yanqi Economic Development Zone C#, Huairou, Beijing, 101407, China
[c] State Key Laboratory of Coal Conversion, Institute of Coal Chemistry, CAS, Taiyuan, 030001, China
[d] SynCat@DIFFER, Syngaschem BV, Eindhoven, 6336 HH, the Netherlands
[e] School of Chemistry, Cardiff University, Park Place, Cardiff, CF10 3AT, UK
[f] Research Institute for Frontier Science, Beihang University, Beijing, 100191, China

ARTICLE INFO

Keywords:
Photo-oxidation of VOC
mixtures Pd cocatalyst
Formaldehyde, toluene and xylenes
Toxic intermediates
Oxygen activation

ABSTRACT

Photocatalytic removal of single volatile organic compounds (VOCs) has been widely investigated; however, photodecomposition of VOC mixtures has been rarely addressed, which may bring safety doubts in indoor air purification due to possible formation of harmful compounds. Here we show that in photocatalytic oxidation of formaldehyde–toluene and formaldehyde–xylene mixtures, the introduction of Pd cocatalyst on TiO_2 photo-catalyst successfully inhibits the formation of toxic methylphenols, thus promoting the complete mineralization of VOC mixtures into CO_2 *via* the harmless benzaldehyde intermediates. Mechanistic analysis reveals that the loading of Pd cocatalyst effectively removes the inherent surface OH groups of TiO_2, which significantly promotes the activation of O_2 into ·OH radicals. The Pd cocatalyst also directs the ·OH radicals to attack the methyl group instead of the aromatic ring for the formation of benzaldehyde and its further oxidation to CO_2, thus yielding a better overall photocatalytic performance.

1. Introduction

As volatile organic compounds (VOCs) are major causes of many chronic lung diseases and cancers [1–3], the development of efficient purification technology as a prerequisite for ensuring high quality in-door air is a subject of ever increasing interest [4–7]. Among various approaches, photocatalysis based processes have attracted great atten-tion for the decomposition of VOCs owing to the following advantages. Firstly, potent oxidizing radicals (*e.g.* ·OH, $\cdot O_2^-$) are formed when the photocatalyst is exposed to irradiation under ambient conditions, which can fully convert most VOC molecules into CO_2 [8–10]. Secondly, there is no need of applying additional oxidants, expensive catalysts, or membranes, adding to its economic potential for applications. Photocatalytic processes are also eminently suitable to deal with relatively low concentrations of pollutants, which makes it ideal for cleaning indoor air to ultimate levels [11–13].

Up to now, the versatility of employing photocatalysis for the decomposition of a wide range of VOCs, including aldehydes and ke-tones, halides, aromatics, has been confirmed by numerous publications [8,9,14–19]. Among these VOCs, formaldehyde and toluene are the most significant and representative toxic compounds, and have been frequently investigated as individual model reactants to evaluate the performance of photocatalysts [20–23]. Photocatalysts ranging from metal oxides (TiO_2, ZnO) to organic polymers (C_3N_4, perylenete-tracarboxylic diimide) and hybrid materials exhibit reasonable effi-ciency even under visible light irradiation [24–28]. Mechanistic studies

* Corresponding author at: Soochow Institute for Energy and Materials InnovationS (SIEMIS), Key Laboratory of Advanced Carbon Materials and Wearable Energy Technologies of Jiangsu Province, Soochow University, Suzhou, 215006, China.
** Corresponding authors.
E-mail addresses: qiaowei@suda.edu.cn (W. Qiao), fengpan@buaa.edu.cn (F. Pan), suren@suda.edu.cn (R. Su).

reveal that photo-dissociation of formaldehyde either undergoes direct oxidation to CO_2 or proceeds *via* an indirect route with formic acid as the intermediate [20,29]. Noticeably, the presence of abundant hydroxyl radicals (·OH) has been identified as the major oxidative species in both cases [30,31]. In the photo-decomposition of toluene, benzaldehyde is observed as the intermediate prior to the cracking of the aromatic ring by the superoxide radicals ($\cdot O_2^-$) [32,33].

However, one should be aware that organic pollutants in realistic indoor and industrial air normally consist of several VOC species from various origins *(e.g.* pesticides, printing inks, furniture, fabrics, adhe-sives, cleaning agents, personal care products and fossil fuels) [34,35]. Representatively, a recent case study on the indoor air quality of an industrial facility by real-time mass spectrometry revealed that a mixture of ethanol, monoterpenes, toluene, and xylenes exist in the at-mosphere [36]. According to our survey of several auditing reports on indoor air analysis, the major VOC components are formaldehyde, toluene, and xylenes [37]. This creates a complicated environment with diverse radicals and reactive intermediates under irradiation, which may result in the formation of more resistive or even toxic compounds. Very recently, Li et al. showed that the presence of formaldehyde can accelerate the decomposition of toluene on SnO_2 photocatalyst; how-ever, the intermediates are plausible and final decomposition products remain unidentified [38]. In general, synergistic or cooperative effects in photo-decomposition of organics has hardly been considered in fundamental investigations, which casts doubts on the applicability of photocatalytic purification of indoor air, and may even imply the exis-tence of potential risks of generating additional harmful compounds.

Herein, we have studied the photocatalytic oxidation of form-aldehyde–toluene and formaldehyde–xylene mixtures using the classic pristine TiO_2 and Pd modified TiO_2 (Pd/TiO_2) photocatalysts. We have assessed photocatalytic performance in terms of apparent removal of pollutant reactants, CO_2 production, and intermediates evolution during photo-dissociation of the mixtures in order to recognize possible safety issues in potential applications. We demonstrate that TiO_2 photo-catalysts convert formaldehyde–toluene and formaldehyde–xylene mixtures partially to toxic intermediates (methylphenols and dimethyl-phenols), while the addition of a Pd cocatalyst prevents their formation and leads to complete decomposition of the organics to CO_2 and H_2O. We present mechanistic investigations to unravel the impact of the Pd cocatalyst on the reaction pathways.

2. Experimental section

2.1. Preparation and characterizations of photocatalysts

All raw materials used in this work were analytical grade without further purification. The pristine TiO_2 is from Evonik Industries AG (Aeroxide® TiO_2, P25). The Pd/TiO_2 with a Pd loading of 1 wt% was synthesized by a modified photo-deposition method [39]. Details of synthetic process is presented in the Supporting Information. The microstructure of the Pd/TiO_2 was characterized by using a spherical-aberration-corrected transmission electron microscope (Cs-corrected TEM, FEI Titan Themis Cubed G2 300). The crystal structure was checked by powder X-ray diffraction (XRD, Bruker AXS D8 Advance diffractometer with a Cu Kα source). The optical properties were analyzed by diffuse reflectance spectroscopy (DRS) using a photo-spectrometer equipped with a spherical integrating detector (UH4150, Hitachi). Spectroscopy grade $BaSO_4$ was employed as the reference. The chemical composition and oxidation states of the ele-ments were analyzed by X-ray photoelectron spectroscopy (XPS) using a Escalab 250Xi spectrometer (Thermo Fisher) equipped with a mono-chromatic Al Ka X-ray source. All binding energy values were calibrated using adventitious carbon at 284.6 eV.

2.2. Photocatalytic VOC decomposition

The apparent photocatalytic performance in removal of formaldehyde-toluene mixtures was evaluated using a home-built in-door air simulator based on a continuous-flow gaseous system (POV-18) equipped with electrochemical sensors, as demonstrated in our previous work and Scheme S1 of the Supporting Information [40]. In brief, 10 mg of photocatalyst powders was deposited on a glass sheet and placed in a quartz tube reactor, which was connected to a 40 L chamber *via* an electromagnetic valve and a flow controller. Then the formaldehyde-toluene mixture vapor was injected into the 40 L chamber *via* a peristaltic pump. When the concentrations of formaldehyde and toluene reached the adsorption-desorption equilibrium, a 365 nm LED light source (10 mW cm ^{2}) was switched on to initiate photocatalytic decomposition of VOC. The initial concentrations of formaldehyde and toluene were identical for comparing pristine TiO_2 and Pd/TiO_2. The in-house relative humidity (RH) was ~50% during all experiments.

The intrinsic photocatalytic performance in complete oxidation of formaldehyde-toluene mixture under in-house humidity conditions (RH: ~50%) was evaluated by following the evolution of gaseous CO_2 using a home-built *in-situ* mass spectrometer (MS) based reaction system (Scheme S2 of the Supporting Information) [41]. Firstly, 10 mg of photocatalyst powders was deposited on a glass petri dish (Φ =25 mm) and placed in the reactor with a volume of 110 cm^3. Then the reaction chamber was immediately sealed after dosing 50 μmol of toluene and 200 μmol of formaldehyde onto the photocatalyst film. A 365 nm LED (10 mW cm ^{2}) was employed to irradiate the reaction chamber for 3 h. The m/e- signals of 44, 32, 28, and 18 were monitored to follow the evolution of CO_2, O_2, N_2, and H_2O simultaneously. Quantification of gas-phase species is realized by applying the ideal gas law, as demon-strated in our previous publications [41]. The photocatalytic decom-position of formaldehyde-xylene mixtures was also performed using the method mentioned above. In addition, the photo-decomposition of formaldehyde-toluene mixture and formaldehyde-xylene mixtures were also evaluated under high humidity conditions (RH = 100%).

2.3. Reaction mechanism analysis

Analysis of the reaction intermediates during photocatalytic decomposition of VOC mixtures was conducted in a 4 mL glass bottle with 10 mg of catalyst deposited onto the bottom at room temperature under ambient conditions under both in-house humidity conditions (RH: ~50%) and high humidity conditions (RH = 100%). Firstly, 2.8 μmol of toluene and 11.2 μmol of formaldehyde were dropped onto the TiO_2 film. Then the glass bottle was sealed and kept in the dark for half an hour to reach adsorption equilibrium prior to 365 nm irradiation. After photocatalytic reaction for 10, 20, 40, and 60 min, 0.5 mL of cyclo-hexane was added into the reaction bottle and sonicated for 15 min to extract the reaction intermediates. The suspension was centrifuged and the aliquots were analyzed by gas chromatography and mass spec-trometry (GC–MS, Agilent 8860 GC system coupled with a 5977B mass selective detector). An HP-5MS column and an FID detector were equipped in the GC–MS.

The *in-situ* attenuated total reflectance Fourier transform infrared spectroscopy (ATR-FTIR) was used to detect the evolution of adsorbed species during the decomposition of VOC mixtures using a Vertex 70 spectrometer (Bruker, Scheme S3 of the Supporting Information). The *in-situ* reaction cell consists of a germanium window and a quartz win-dow to allow UV light passing through. A 10 mg photocatalyst was deposited on the Ge window and the spectrum is recorded as back-ground. After the acetaldehyde-toluene mixture was dropped on the surface of the photocatalyst film under dark conditions, the cell is closed to avoid evaporations. Here formaldehyde is replaced by acetaldehyde to avoid the presence of water into the system, therefore the formation of possible hydroxyl species and water can be identified from the IR spectra. The 365 nm irradiation (10 mW cm ^{2}) was applied for 3 h after

the adsorption of VOC mixtures reached an equilibrium. FTIR spectra in the range of 3800 900 cm ^{1} were continuously collected every 5 min. More experimental details can be found in our previous work and the Supporting Information [41].

The radicals generated during the photo-decomposition of VOCs were analyzed by electron paramagnetic resonance (EPR) using an X-band JES-X320 spectrometer in the range of 320–340 mT at room temperature (RT). A modulation width of 0.12 mT and an receiver gain of 200 was used for all measurements. Firstly, a 10 mg of photocatalyst powders was dispersed in 1 mL of dimethyl sulfoxide (DMSO) that contains 5 mM of paraformaldehyde and toluene. Here para-formaldehyde was employed to avoid the addition of water. Prior to analysis, the spin-trap solution (30 mM of N-tert-butyl-α-phenylnitrone, PBN, or 5-tert-butoxycarbonyl-5-methyl-1-pyrroline-N-oxide, BMPO) was dosed into the catalyst-reactant suspension and exposed to UV irradiation (365 nm) at room temperature for 0.5 min. In parallel, the spin-trap EPR analysis was also conducted using toluene as the solvent and otherwise identical experimental conditions.

3. Results and discussion

3.1. Apparent and intrinsic photocatalytic performances

Fig. 1 shows the apparent removal of formaldehyde–toluene mixture with a molar ratio of 4:1 by using a conventional electrochemical sensor based method under RH of 50% [40]. This ratio is believed to be representative for contaminated indoor air [42]. Details of the pristine TiO_2 (Degussa P25) and Pd/TiO_2 photocatalysts prepared *via* photo-deposition process are listed in the Supporting Information (Fig. S1). Upon UV irradiation, pristine TiO_2 and Pd/TiO_2 show very similar conversion rates for the removal of both formaldehyde (Fig. 1a) and toluene (Fig. 1b). A slightly slower kinetics is observed for the removal of toluene compared to that of formaldehyde, which is associ-ated to the stability of the aryl ring. The Pd cocatalyst seems to have a negligible effect in the removal of formaldehyde–toluene mixture, however, it should be noted that the measurement only represents the consumption of reactants *via* electrochemical sensors (Fig. 1c), while the identity of the oxidized products and the level of mineralization remain unclear.

To evaluate the intrinsic performance of the photocatalysts in oxidation of toluene–formaldehyde mixture, *in-situ* mass spectrometry (MS) is employed to monitor the formation of CO_2 (Figs. 2 and S3 in the Supporting Information). Surprisingly, Pd/TiO_2 exhibits a ~2 times higher CO_2 production than that of pristine TiO_2 within 3 h of irradia-tion under RH of 50% (Fig. 2a). Since both photocatalysts show similar light absorption within the UV range (Fig. S1 in the Supporting Infor-mation), it is considered that the presence of Pd cocatalyst promotes the complete oxidation of formaldehyde and toluene, whereas pristine TiO_2 decomposes the mixture only partially to CO_2, most likely accompanied with oxygenated intermediates. Besides, the Pd/TiO_2 exhibits decent stability for the photodecomposition of formaldehyde–toluene mixtures within 4 consecutive cycles. *Post-mortem* analysis of the spent Pd/TiO_2 confirms that the size and oxidation states of the metallic Pd NPs re-mains unchanged (Fig. S2 in the Supporting Information). Furthermore, Fig. 2(b) and (c) depict the intrinsic efficiencies of pristine TiO_2 and Pd/ TiO_2 in photocatalytic decomposition of formaldehyde–xylene mixtures

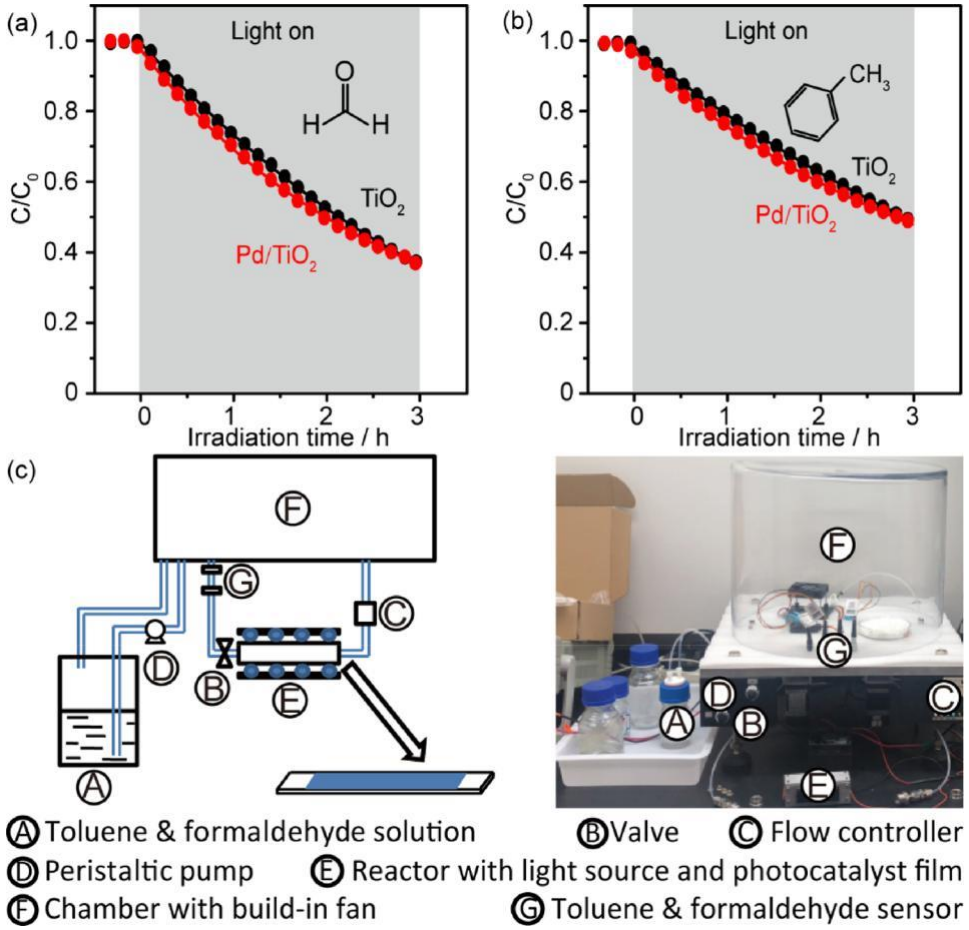

Fig. 1. Apparent removal of **(a)** formaldehyde and **(b)** toluene during photocatalytic decomposition of a formaldehyde–toluene mixture using pristine TiO_2 and Pd/ TiO_2 determined by an electrochemical sensor-based method. Reaction conditions: formaldehyde/toluene in 4:1 M ratio, 10 mg photocatalyst, 365 nm LED (10 mW·cm ^{2}, 3 h), RH = 50%. **(c)** Diagram and image of the sensor-based setup for determining the apparent photo-removal of VOCs.

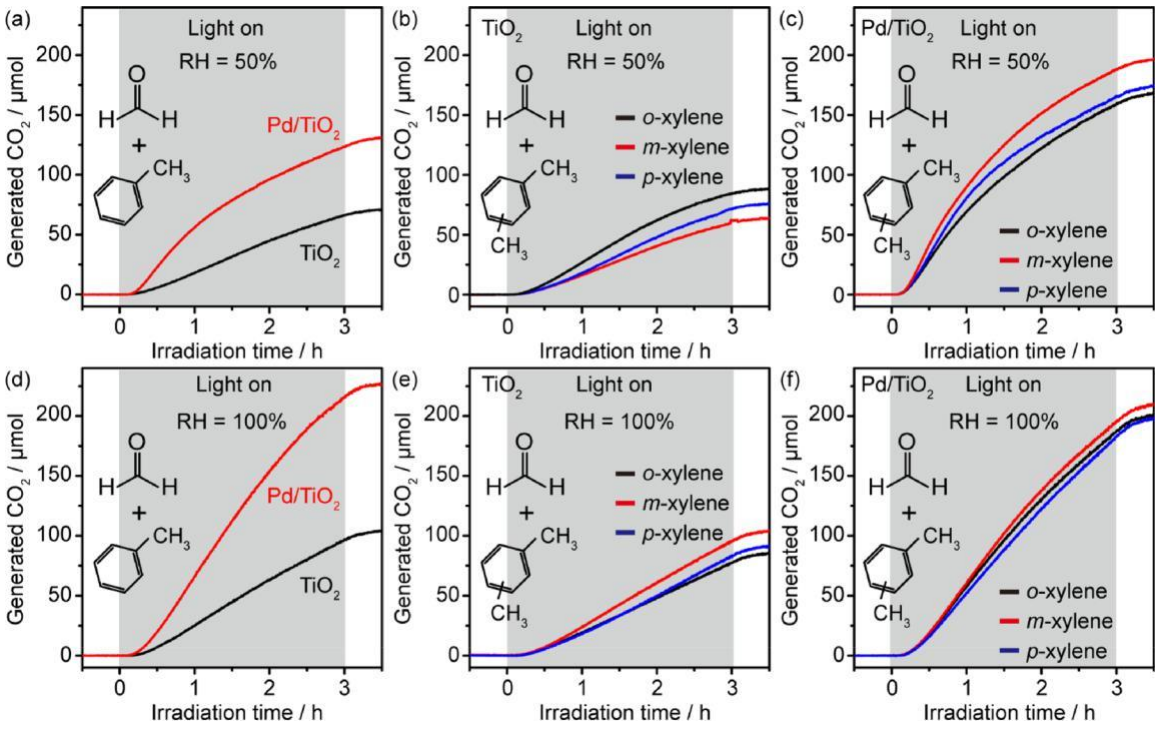

Fig. 2. CO 2 evolution in photocatalytic decomposition of formaldehyde–toluene and formaldehyde–xylene mixtures using pristine TiO_2 and Pd/TiO_2 determined by *in-situ* MS. **(a)-(c),** at RH = 50%, **(d)-(f),** at RH = 100%, respectively. Reaction conditions: 200 *μ*mol of formaldehyde and 50 *μ*mol of toluene (xylenes), 10 mg photocatalyst, 365 nm LED (10 mW·cm ^{2}, 3 h).

under RH of 50%. When pristine TiO_2 is employed as the photocatalyst, a similar CO_2 generation rate of ~20 *μ* mol h ^{1} and a total mass pro-duction of ~60 *μ*mol is observed within 3 h for the decomposition of formaldehyde *o*-xylene, *m*-xylene, and *p*-xylene mixtures, respec-tively (Fig. 2b). In contrast, 2~3.5-times enhancement in CO_2 evolution is observed when Pd/TiO_2 is used as the photocatalyst for the decom-position of all formaldehyde–xylene mixtures under RH of 50% (Fig. 2c), again confirming the key role of the Pd cocatalyst.

Additionally, the Pd/TiO_2 also outperforms pristine TiO_2 under a higher environmental humidity in decomposition of form-aldehyde–toluene and formaldehyde–xylene mixtures (RH = 100%, Fig. 2d–f). A significant enhancment in CO_2 evolution rate is observed for both Pd/TiO_2 and TiO_2 in decomposition of formaldehyde–toluene upon increasing humidity, indicating that an increased adsorption of H_2O promotes the formation of ·OH radicals, thus resulting in a fast decomposition of the VOCs mixture. The phenomenon is less obvious for the photodecomposition of formaldehyde–xylene mixtures, suggesting that an optimum photocatalytic performance of Pd/TiO_2 is achieved. The improved photo-oxidation efficiency of formaldehyde–toluene may associate to the increased photo-generation rate of hydroxyl radicals (·OH) under a higher water concentration, whereas the little improve-ment in photo-dissociation of formaldehyde–xylene indicates that the formation rate of ·OH is no longer the rate limiting step (RDS) for the oxidation of xylenes.

3.2. Identification of intermediates and by-products

The similar trend observed in all cases indicates that Pd cocatalyst is essential in the complete photo-dissociation of formaldehyde toluene and formaldehyde–xylenes mixtures. Therefore, the possible in-termediates and by-products during photocatalytic decomposition of formaldehyde–toluene mixtures are probed to reveal the mechanisms by using gas chromatograph-mass spectroscopy (GC–MS). With toluene as the only reactant, benzaldehyde is observed as the solely stable inter-mediate for both pristine TiO_2 and Pd/TiO_2 (retention time [rt] =2.582 min, Fig. S7 in the Supporting Information). Kinetic analysis shows that pristine TiO_2 and Pd/TiO_2 exhibit a similar formation rate of benzal-dehyde, and the presence of Pd cocatalyst only slightly enhances the decomposition rate of benzaldehyde (Fig. S7 in the Supporting Information).

Interestingly, distinct intermediates are observed during the photo-catalytic process when formaldehyde and toluene are injected simulta-neously under a RH of 50% (Fig. 3a). When pristine TiO_2 is used as the photocatalyst, the slow decomposition of toluene is accompanied with the formation and accumulation of *o*-methylphenol (rt =3.494 min) and *m*-methylphenol (rt =3.806 min) in the early stage of the irradiation process (t < 20 min, Figs. 3a and S8 in the Supporting Information). Simultaneously, benzaldehyde starts to evolve after the concentration of methylphenols reaches an equilibrium. Since methylphenols are highly toxic chemicals with potential risk to the environment and human or-gans [43,44], the photocatalytic process employing pristine TiO_2 is not appropriate for indoor air purification applications. In comparison, the Pd/TiO_2 not only presents a fast decompositon rate of toluene, but also supresses the formation of toxic methylphenols with benzaldehyde as the sole intermediate over the whole irradiation course, which offers a safe and efficient solution for the removal of VOCs mixtures. In addition, while the concentration of benzaldehyde builds-up slowly and reaches a plateau for pristine TiO_2, the formation of benzaldehyde and the consecutive dissociation step for Pd/TiO_2 are only slightly slower compared to the case of pure toluene (Fig. S7 in the Supporting Infor-mation). This suggests that the formation of methylphenols may hinder the complete oxidation of toluene into CO_2. At a higher humidity (RH = 100%), the pristine TiO_2 exhibits a reduced photo-conversion rate of toluene and a slower formation rate of both methylphenols and benz-aldehyde (Fig. 3b). In contrast, the removal rate of toluene using Pd/TiO_2 remains almost unchanged at high humidity. Additionally, while a tiny increase in methylphenol formation is observed for Pd/TiO_2 , the formation of benzaldehyde is completely surpressed under high humidity conditions. In consideration with the increased CO_2 for-mation rates under high humidity conditions, it indicates that the

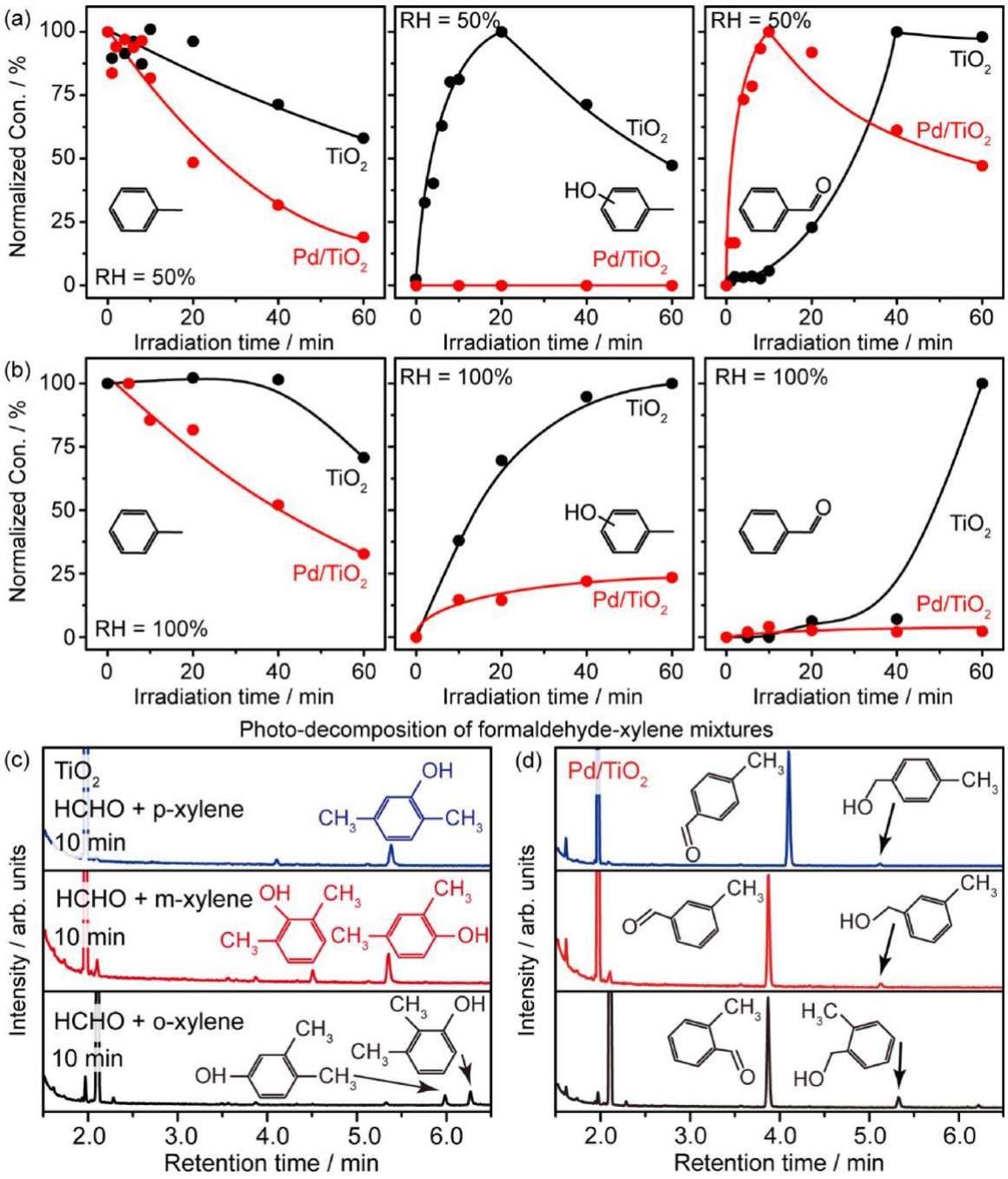

Fig. 3. Probe of reaction intermediates. **(a)** and **(b)** Evolution of toluene, methylphenols, and benzaldehyde during photo-decomposition of formaldehyde-toluene mixture using TiO_2 and Pd/TiO_2 at RH of 50% and 100%. **(c)** and **(d)** GC–MS analysis of the reaction intermediates during photo-decomposition of formaldehyde-xylene mixtures using pristine TiO_2 and Pd/TiO_2.

photo-generated ·OH radicals on TiO_2 tend to attack toluene in the order of aryl C–H bond, methyl group, and ring opening, resulting in severe accumulation of partially oxidized products. The addition of Pd cocat-alyst directs the utilization of ·OH radicals to attack the methyl group and accelerates the overall oxidation of toluene to produce CO_2.

Nevertheless, a similar trend is also observed during photocatalytic dissociation of formaldehyde–*p*-xylene, formaldehyde–*m*-xylene, and formaldehyde–*o*-xylene mixtures under a RH of 50% (Fig. 3c and d). While the accumulation of corresponding dimethyl-phenols is observed in the early stage using pristine TiO_2 photocatalyst (Figs. 3c and S9 in the Supporting Information), methyl-benzaldehydes and trace amount of corresponding methylbenzyl alcohols are the major intermediates when Pd/TiO_2 is used as the photocatalysts (Figs. 3d and S9 in the Supporting Information).

The origin of different intermediates/by-products and the impact of Pd cocatalyst have been further explored by control experiments and *in-situ* vibrational spectroscopy. Initially, the formation of methylphenols on pristine TiO_2 caused by water in the formaldehyde has been ruled out. When formaldehyde is replaced by an equivalent amount of water in the photocatalytic system, benzaldehyde becomes the solely detect-able intermediate during toluene dissociation within the whole irradi-ation courses for both pristine TiO_2 and Pd/TiO_2 (Figs. 4a and S10 in the Supporting Information). Since it has been observed that large amounts of ·OH radicals are generated during photodissociation of formaldehyde [30,31], it is reasonable to consider that the formation of methylphenols and dimethyl phenols originates from the attacking of ·OH radicals on

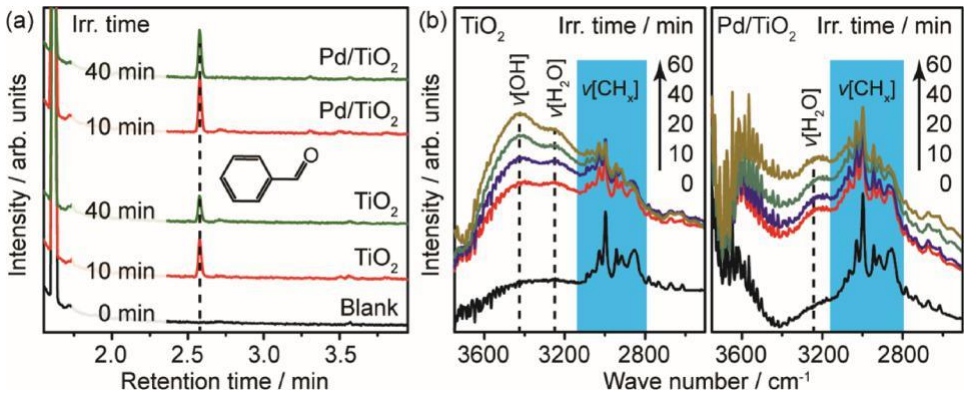

Fig. 4. Verification of reaction mechanisms. **(a)** GC analysis of intermediates during photo-decomposition of toluene in the presence of water. **(b)** *In-situ* FTIR analysis recorded during photo-decomposition of an acetaldehyde–toluene mixture using pristine TiO_2 and Pd/TiO_2.

the aromatic ring of toluene and dimethylbenzenes, respectively. In contrast, the presence of Pd results in the direct activation of molecular O_2 [45], which is more likely to attack the methyl group and enables the formation of corresponding aldehydes. This view is supported by infrared spectroscopy, as we discuss hereafter.

Figs. 4b and S11 in the Supporting Information show *in-situ* FTIR spectra of an acetaldehyde–toluene mixture under irradiation in the presence of pristine TiO_2 and Pd/TiO_2. Here acetaldehyde is used instead of formaldehyde to avoid the interference of water in the re-agent. When TiO_2 is used as the photocatalyst, two vibrational peaks in the O –H stretch region evolve gradually upon irradiation, which can be assigned to the hydroxyl group (OH) of methylphenol (3410 cm ^{1}) and water (3250 cm ^{1}) [42]. This indicates that the aldehyde is involved in the activation of O_2 to produce ·OH radicals. In contrast, only the formation of water (3250 cm ^{1}) is observed in the corresponding spectra of the acetaldehyde–toluene mixture on Pd/TiO_2 under irradiation, suggesting that the activation of O_2 either undergoes a rapid consump-tion of ·OH radicals or *via* the $·O_2$- radical. Fig. 4b also shows that during irradiation the CH_x vibrational peaks from toluene and acetaldehyde decrease, confirming their photodecomposition.

3.3. Active species detection and promotion mechanism of Pd

The identity of long-lifetime radicals in photocatalytic decomposi-tion of formaldehyde, toluene, and their mixtures are explored by add-ing the 2,2,6,6-tetramethylpiperidinyloxy (TEMPO) in the reaction system (Figs. 5a, b and S12 in the Supporting Information). With pristine TiO_2 as the photocatalyst and formaldehyde as the sole reactant, mainly trapped H species (rt =4.670 min) and unreacted TEMPO (rt =5.176 min) are observed (Fig. 5a, black curve). According to previous inves-tigation [46], the trapped H species originate from the C–H bond dissociation of formaldehyde (Eq. 1). In comparison, no obvious in-termediates are detected during photo-dissociation of toluene (red curve of Fig. 5a). Interestingly, an additional species (rt =2.353 min) appears during photocatalytic decomposition of the formaldehyde–toluene mixture (blue curve of Figs. 5a and S12 in the Supporting Information).

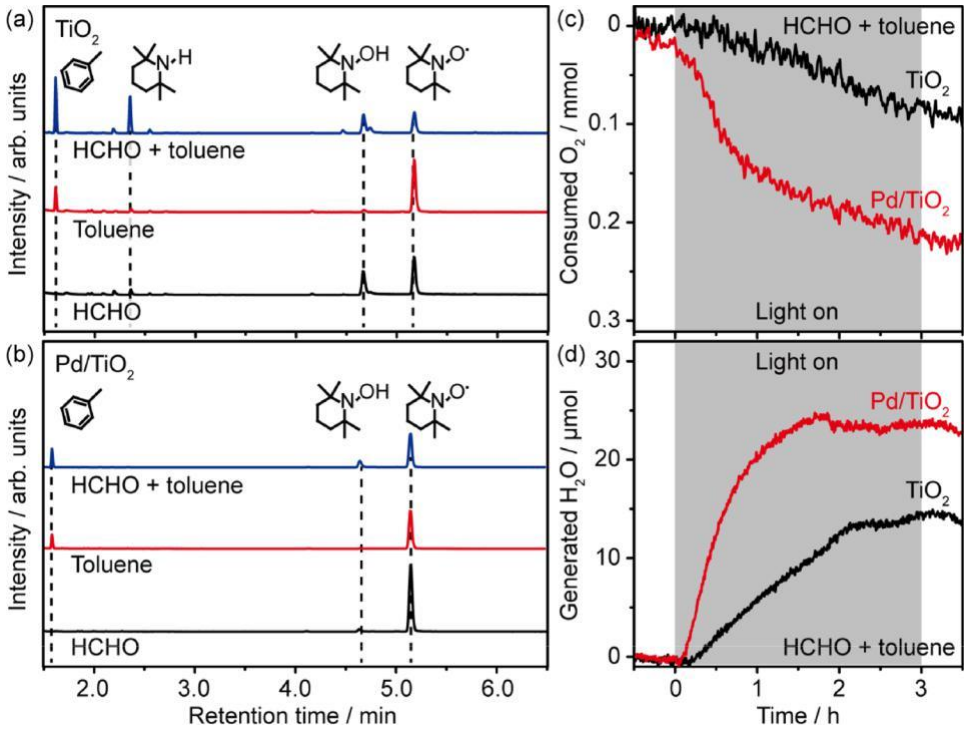

Fig. 5. (a) and **(b)** GC–MS analysis of radical species during photo-decomposition of a formaldehyde–toluene mixture using TEMPO (80 mM) as a radical trap. **(c)** and **(d)** *In-situ* MS analysis of O_2 consumption and water formation during photo-decomposition of a formaldehyde–toluene mixture using pristine TiO_2 and Pd/TiO_2.

This species derives most likely from the ·OH radical acctacking of TEMPO, which undergoes subsequent removal of ·OOH radical and hydrogen addition from formaldehyde or toluene according to Eq. (2) [46]. In comparison, only trace amount of H species are observed when Pd/TiO_2 is used as the photocatalyst in the presence of formaldehyde (Fig. 5b, black and blue curve). These results indicate that the photo-generated ·OH radicals on pristine TiO_2 are more prone to be trapped with TEMPO instead of interacting with formaldehyde and toluene, whereas Pd/TiO_2 can use the ·OH radicals more efficiently to decompose formaldehyde and toluene.

The divergence in formation and utilization of ·OH radicals between pristine TiO_2 and Pd/TiO_2 also indicates that the two photocatalysts exhibit different features upon activation of molecular oxygen, as revealed by *in-situ* MS of the consumed O_2 and generated H_2 O (Fig. 5c and d). When pristine TiO ₂ is used as the photocatalyst, a total amount of ~80 μmol O_2 is reduced within 3 h of irradiation in the presence of formaldehyde–toluene mixture. In comparison, Pd/TiO_2 exhibits a much faster O_2 consumption rate (~220 μmol within 3 h) during photode-composition of formaldehyde–toluene mixture compared to that of pristine TiO_2 (Fig. 5c), indicating a more efficient utilization of the photogenerated charge carriers, and thus providing a faster decompo-sition rate of the pollutants. Correspondingly, the Pd/TiO_2 also shows a faster formation rate of water compared to that of pristine TiO_2 (Fig. 5d), suggesting that the Pd cocatalyst facilitates the efficient utilization of photogenerated ·OH radicals. Additionally, since Pd is a promising catalyst in dehydrogenation reactions [47], it may also promote direct conversion of O_2 into H_2O *via* abstraction of H from the methyl group of toluene and dimethylbenzene, thus avoiding the formation of the toxic cresolic intermediates.

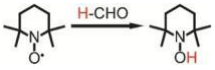

(1)

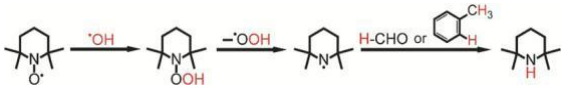

(2)

The effect of the Pd cocatalyst on tuning the pathways of photo-degradation formaldehyde-toluene mixture has been further elucidated by EPR analysis of the short lifetime radicals, as shown in Fig. 6. The liquid-phase EPR analysis can be considered as an extreme of high hu-midity reaction conditions. The pristine TiO_2 and Pd/TiO_2 show different surface features under dark conditions, as revealed by using DMSO as the solvent and PBN as the spin-trap (black curves in Fig. 6a and b). Prior to irradiation, the EPR spectra of pristine TiO_2 are well reproduced by one radical species, which can be assigned to the ·OH radical ($a[^1$ H] = 6.41 and $a[^{14}$N] =38.83 MHz) that originates from the hydroxylated surface (OH) of pristine TiO_2 [48]. In contrast, the Pd/TiO_2 only shows very weak signals of ·OH radical, indicating that the surface OH of TiO_2 are mostly removed after Pd modification. It also suggests that the surface OH of pristine TiO_2 may account for the formation of methylphenolics during photodegradation of toluene.

After irradiation of the catalyst suspension for 0.5 min, the EPR spectra of both pristine TiO_2 and Pd/TiO_2 are resolved by an identical radical ($a[^1$H] = 8.67 and $a[^{14}$N] =42.60 MHz), regardless of only formaldehyde or formaldehyde-toluene mixture as the reactant (red and blue curves in Fig. 6a and b). This new signal is assigned to the ·CH_3 radical due to the well-known conversion of ·OH into ·CH_3 *via* reaction with DMSO (Eq. 3) [49]. No other oxygen radical species is observed (*i. e.*, superoxide radical and singlet oxygen). BMPO has been also employed as the spin-trap to check the existence of other oxygen radicals with short lifetimes, and only ·OH radical is observed (Fig. S13 in the Supporting Information). In addition, it should be also noted that similar intensities of ·OH radical are observed for both TiO_2 and Pd/TiO_2 upon irradiation in the presence of formaldehyde or formaldehyde-toluene mixture, suggesting that the surface modification of TiO_2 by Pd cocat-alyst does not change the formation pathways of oxygen radical species.

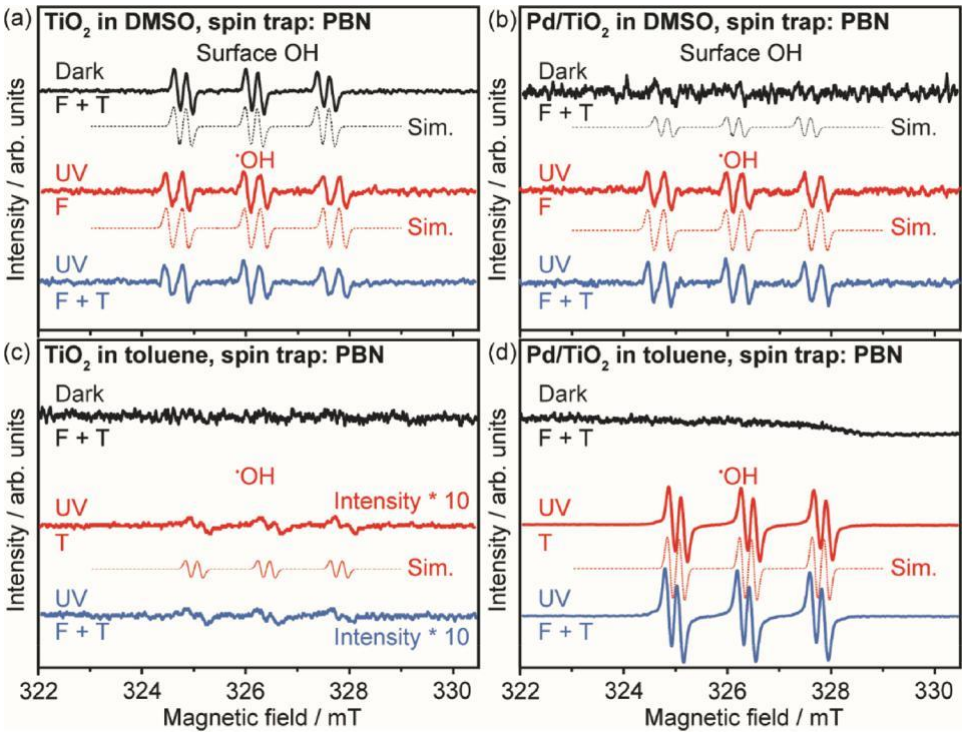

Fig. 6. EPR spectra of irradiated photocatalyst suspensions in the presence of formaldehyde (F, 5 mM), toluene (T, 1.5 mM) and formaldehyde toluene mixture (F + T) under aerated conditions at RT. **(a)** and **(b)** pristine TiO_2 and Pd/TiO_2 in DMSO solvent using PBN as the spin-trap; **(c)** and **(d)** pristine TiO_2 and Pd/TiO_2 in toluene solvent using PBN as the spin-trap. The irradiation time is 0.5 min for all measurements. Dashed spectra are corresponding simulations.

$(CH_3)_2SO + {}^{\cdot}OH \rightarrow CH_3SO_2H + {}^{\cdot}CH_3$ (3)

Interestingly, a significant change of the EPR spectra is observed when toluene is employed as the solvent instead of DMSO (Fig. 6c and d). Note that this analysis is closer to realistic reaction conditions, where only VOC compound(s) and molecular oxygen are involved. Prior to irradiation, no EPR signal is detected for both photocatalysts with PBN as the spin-trap (black curves in Fig. 6c and d). Upon irradiation, while a very weak contribution of ·OH radicals ($a[^1H]$ = 6.23 and $a[^{14}N]$ =39.05 MHz) is observed for pristine TiO_2 upon irradiation in the presence of toluene or formaldehyde toluene mixture (red and blue curves in Fig. 6c), very intense ·OH radical signals appear for Pd/TiO_2 (red and blue curves in Fig. 6d). Since the concentration of toluene (9.4 M) is significantly greater than that of formaldehyde (5 mM) and dissolved O_2 (~15 ppm), it indicates that the presence of the Pd cocatalyst strongly enhances the activation of molecular oxygen under high pollutant con-centration compared to that of pristine TiO_2. Nevertheless, the addition of formaldehyde does not change the radical species for Pd/TiO_2, indi-cating the decomposition path remains unchanged.

Based on the analysis of reaction intermediates and kinetics, we have proposed the reaction mechanism shown in Scheme 1. When pristine TiO_2 is used as the photocatalyst, surface OH group together with photogenerated ·OH radicals attack the aromatic ring of toluene and xylenes to produce the corresponding methylphenols and dimethyl-phenols, which are categorized as corrosive, acutely toxic, and envi-ronmentally dangerous according to the Globally Harmonized System of classification and labeling of chemicals (GHS). Although methylphenols and dimethylphenols can be photo-decomposed to CO_2, slower reaction kinetics is expected due to their stability. In contrast, surface modifi-cation of Pd results in the removal of OH groups on TiO_2 and signifi-cantly promotes the formation of active oxygen radicals under high VOC concentrations. This in turn accelerates the dissociation of toluene and xylenes to produce corresponding aromatic aldehydes and ring-opening products, thus avoiding the formation of methylphenolics. Moreover, they are easier to be decomposed, thus providing a preferred route for the dissociation of formaldehyde–toluene and formaldehyde–xylene VOC mixtures.

4. Conclusion

Here, we have studied the photocatalytic oxidation of form-aldehyde–toluene and formaldehyde–xylene mixtures to examine the catalytic process from both application and fundamental aspects. When pristine TiO_2 is employed as the photocatalyst, toxic and stable meth-ylphenols are produced due to the surface OH group and photo-generated ·OH radicals on TiO 2. The formation of toxic methylphenols can be inhibited by modifying pristine TiO 2 with Pd cocatalyst, which dissociates the formaldehyde–toluene and formaldehyde–xylene mix-tures at a much faster rate *via* the formation of less toxic benzaldehydes. The intrinsic surface OH group of pristine TiO_2 results in a poor ac-tivity in photogeneration of ·OH radicals and directs selective attacking of the aromatic ring for the formation of phenolic species. In compari-son, the loading of Pd cocatalyst removes the surface OH groups on TiO_2 and accelerates the direct activation of O 2 into ·OH radicals, which promotes the oxidation of the methyl group of toluene and xylenes, thus favoring the formation of aromatic aldehydes and their degradation to CO_2, yielding a much better overall performance. Alternative strategies (*i.e.*, construct heterojunctions and surface oxygen vacancies) that may achieve this goal should be explored to design noble metal free photocatalysts.

Author contributions

RS conceived the studies. QW synthesized the samples; QW, WQ, and FP performed the photocatalytic tests; QW and WQ carried out the material characterizations. All authors were involved in the design of the experiments, the discussion of the results, and the writing of the manuscript.

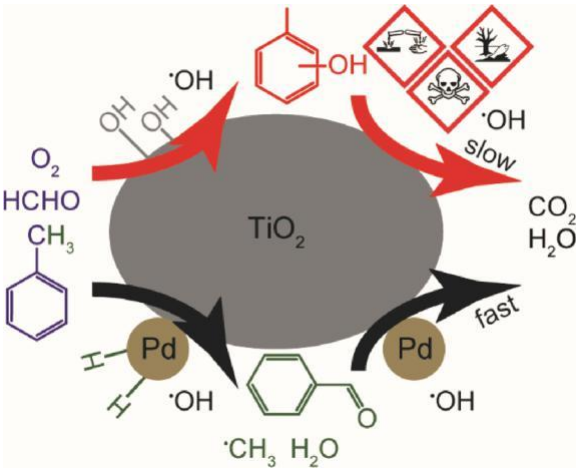

Scheme 1. Proposed reaction scheme for the photocatalytic decomposition of formaldehyde–toluene mixture using pristine TiO_2 and Pd/TiO_2. The photo-decomposition of formaldehyde–xylene mixtures proceed *via* similar steps.

CRediT authorship contribution statement

Qiqi Wu: Investigation, Formal analysis, Visualization, Writing - review & editing. **Jiani Ye:** Investigation, Formal analysis. **Wei Qiao:** Investigation, Formal analysis, Visualization, Writing - review & editing. **Yongwang Li:** Resources. **J.W. (Hans) Niemantsverdriet:** Resources, Writing - review & editing. **Emma Richards:** Formal analysis, Data curation. **Feng Pan:** Methodology, Resources. **Ren Su:** Conceptualiza-tion, Methodology, Validation, Resources, Writing - original draft, Writing - review & editing, Supervision, Funding acquisition.

Declaration of Competing Interest

The authors report no declarations of interest.

Acknowledgments

RS would like to thank the NSFC (project number: 21972100), the Priority Academic Program Development of Jiangsu Higher Education Institutions (PAPD, project number: NH10800120) for financial support. ER thanks financial support from EPSRC (EP/T013079/1). RS, JWN and Syngaschem BV acknowledge significant funding from Synfuels China Technology Co. Ltd.

Appendix A. Supplementary data

References

[1] K. Rumchev, H. Brown, J. Spickett, Volatile organic compounds: do they present a risk to our health? Rev. Environ. Health 22 (2007) 39–55.
[2] P. Kongtip, W. Thongsuk, W. Yoosook, S. Chantanakul, Health effects of metropolitan traffic-related air pollutants on street vendors, Atmos. Environ. 40 (2006) 7138–7145.
[3] H. Guo, S.C. Lee, L.Y. Chan, W.M. Li, Risk assessment of exposure to volatile organic compounds in different indoor environments, Environ. Res. 94 (2004) 57–66.
[4] A. Luengas, A. Barona, C. Hort, G. Gallastegui, V. Platel, A. Elias, A review of indoor air treatment technologies, Rev. Environ. Sci. Biotechnol. 14 (2015) 499–522.
[5] J.M. Molina-Jorda,´ Highly adsorptive and magneto-inductive guefoams (multifunctional guest-containing foams) for enhanced energy-efficient preconcentration and management of VOCs, ACS Appl. Mater. Interfaces 12 (2020) 11702–11712.

[6] R.A. Raso, M. Zeltner, W.J. Stark, Indoor air purification using activated carbon adsorbers: regeneration using catalytic combustion of intermediately stored VOC, Ind. Eng. Chem. Res. 53 (2014) 19304–19312.

[7] J.Y. Chen, D.L. Zhang, G.Y. Li, T.C. An, J.M. Fu, The health risk attenuation by simultaneous elimination of atmospheric VOCs and POPs from an e-waste dismantling workshop by an integrated de-dusting with decontamination technique, Chem. Eng. J. 301 (2016) 299–305.

[8] X.Y. Wu, X.Y. Wang, J. Li, G.K. Zhang, Boosting molecular oxygen activation of $SrTiO_3$ by engineering exposed facets for highly efficient photocatalytic oxidation, J. Mater. Chem. A 5 (2017) 23822–23830.

[9] Y.Y. Wang, C.Z. Yang, A. Chen, W.H. Pu, J.Y. Gong, Influence of yolk-shell Au@ TiO_2 structure induced photocatalytic activity towards gaseous pollutant degradation under visible light, Appl. Catal. B: Environ. 251 (2019) 57–65.

[10] J.Y. Chen, Z.G. He, Y.M. Ji, G.Y. Li, T.C. An, W.Y. Choi, •OH radicals determined photocatalytic degradation mechanisms of gaseous styrene in TiO_2 system under 254 nm versus 185 nm irradiation: combined experimental and theoretical studies, Appl. Catal. B: Environ. 257 (2019), 117912.

[11] R.B. Sun, Z.G. Xi, F.H. Chao, W. Zhang, H.S. Zhang, D.F. Yang, Decomposition of low-concentration gas-phase toluene using plasma-driven photocatalyst reactor, Atmos. Environ. 41 (2007) 6853–6859.

[12] J. Zhao, X.D. Yang, Photocatalytic oxidation for indoor air purification: a literature review, Build. Environ. 38 (2003) 645–654.

[13] J.H. Mo, Y.P. Zhang, Q.J. Xu, J.J. Lamson, R.Y. Zhao, Photocatalytic purification of volatile organic compounds in indoor air: a literature review, Atmos. Environ. 43 (2009) 2229–2246.

[14] J.W. Tang, Z.G. Zou, J.H. Ye, Efficient photocatalytic decomposition of organic contaminants over $CaBi_2O_4$ under visible-light irradiation, Angew. Chem. Int. Ed. 43 (2004) 4463–4466.

[15] X. Chen, H.Y. Zhu, J.C. Zhao, Z.F. Zheng, X.P. Gao, Visible-light-driven oxidation of organic contaminants in air with gold nanoparticle catalysts on oxide supports, Angew. Chem. Int. Ed. 47 (2008) 5353–5356.

[16] Q.J. Xiang, K.L. Lv, J.G. Yu, Pivotal role of fluorine in enhanced photocatalytic activity of anatase TiO_2 nanosheets with dominant (001) facets for the photocatalytic degradation of acetone in air, Appl. Catal. B: Environ. 96 (2010) 557–564.

[17] Y.F. Zhang, S.J. Park, Bimetallic AuPd alloy nanoparticles deposited on MoO_3 nanowires for enhanced visible-light driven trichloroethylene degradation, J. Catal. 361 (2018) 238–247.

[18] Y.D. Hou, L. Wu, X.C. Wang, Z.X. Ding, Z.H. Li, X.Z. Fu, Photocatalytic performance of α-, β-, and γ -Ga_2O_3 for the destruction of volatile aromatic pollutants in air, J. Catal. 250 (2007) 12–18.

[19] C.L. Bianchi, G. Cappelletti, S. Ardizzone, S. Gialanella, A. Naldoni, C. Oliv, C. Pirola, N-doped TiO_2 from $TiCl_3$ for photodegradation of air pollutants, Catal. Today 144 (2009) 31–36.

[20] J.Y. Li, W. Cui, P. Chen, X.A. Dong, Y.H. Chu, J.P. Sheng, Y.X. Zhang, Z.M. Wang, F. Dong, Unraveling the mechanism of binary channel reactions in photocatalytic formaldehyde decomposition for promoted mineralization, Appl. Catal. B: Environ. 260 (2020), 118130.

[21] S. Ardizzone, C.L. Bianchi, G. Cappelletti, A. Naldoni, C. Pirola, Photocatalytic degradation of toluene in the gas phase: relationship between surface species and catalyst features, Environ. Sci. Technol. 42 (2008) 6671–6676.

[22] J.Y. Li, X.A. Dong, G. Zhang, W. Cui, W.L. Cen, Z.B. Wu, S.C. Lee, F. Dong, Probing the ring-opening pathways for efficient photocatalytic toluene decomposition, J. Mater. Catal. A 7 (2019) 3366–3374.

[23] J.H. Mo, Y.P. Zhang, Q.J. Xu, Y.F. Zhu, J.J. Lamson, R.Y. Zhao, Determination and risk assessment of by-products resulting from photocatalytic oxidation of toluene, Appl. Catal. B: Environ. 89 (2009) 570–576.

[24] X.B. Zhu, C. Jin, X.S. Li, J.L. Liu, Z.G. Sun, C. Shi, X.G. Li, A.M. Zhu, Photocatalytic formaldehyde oxidation over plasmonic Au/TiO_2 under visible light: moisture indispensability and light enhancement, ACS Catal. 7 (2017) 6514–6524.

[25] E. Kowalskaa, K. Yoshiiri, Z.S. We, S.Z. Zheng, E. Kastlc, H. Remitad, B. Ohtani, S. Rau, Hybrid photocatalysts composed of titania modified with plasmonicnanoparticles and ruthenium complexes for decomposition of organiccompounds, Appl. Catal. B: Environ. 178 (2015) 133–143.

[26] J.O. Saucedo-Lucero, S. Arriaga, Study of ZnO-photocatalyst deactivation during continuous degradation of n-hexane vapors, J. Photochem. Photobiol. A 312 (2015) 28–33.

[27] Y.H. Li, Y.J. Sun, W.K. Ho, Y.X. Zhang, H.W. Huang, Q. Cai, F. Dong, Highly enhanced visible-light photocatalytic NO_x purification and conversion pathway on self-structurally modified g-C_3N_4 nanosheets, Sci. Bull. 63 (2018) 609–620.

[28] W.G. Zeng, T. Cai, Y.T. Liu, L.L. Wang, W.Y. Dong, H. Chen, X.N. Xia, An artificial organic-inorganic Z-scheme photocatalyst WO_3@Cu@PDI supramolecular with excellent visible light absorption and photocatalytic activity, Chem. Eng. J. 381 (2020), 122691.

[29] G.X. Zhang, Z.M. Sun, Y.W. Duan, R.X. Ma, S.L. Zheng, Synthesis of nano-TiO_2/ diatomite composite and its photocatalytic degradation of gaseous formaldehyde, Appl. Surf. Sci. 412 (2017) 105–112.

[30] N. He, Z.H. Li, Palladium-atom catalyzed formic acid decomposition and the switch of reaction mechanism with temperature, Phys. Chem. Chem. Phys. 18 (2016) 10005–10017.

[31] C.S. Huang, C.M. Zhang, X.M. Yang, State-selected imaging studies of formic acid photodissociation dynamics, J. Chem. Phys. 132 (2010), 154306.

[32] Z.Y. Sheng, D.R. Ma, Q. He, K. Wu, L. Yang, Mechanism of photocatalytic toluene oxidation with $ZnWO_4$: a combined experimental and theoretical investigation, Catal. Sci. Technol. 9 (2019) 5692–5697.

[33] S.M. Liang, Y.J. Shu, K. Li, J. Jian, H.B. Huang, J.G. Deng, D.Y.C. Leungd, M.Y. Wu, Y.G. Zhang, Mechanistic insights into toluene degradation under VUV irradiation coupled with photocatalytic oxidation, J. Hazard. Mater. 399 (2020), 122967.

[34] T. Salthammer, Very volatile organic compounds: an understudied class of indoor air pollutants, Indoor Air 26 (2016) 25–38.

[35] B.C. McDonald, J.A. de Gouw, J.B. Gilman, S.H. Jathar, A. Akherati, C.D. Cappa, J. L. Jimenez, J. Lee-Taylor, P.L. Hayes, S.A. McKeen, Y.Y. Cui, S.W. Kim, D. R. Gentner, G. Isaacman-VanWertz, A.H. Goldstein, R.A. Harley, G.J. Frost, J. M. Roberts, T.B. Ryerson, M. Trainer, Volatile chemical products emerging as largest petrochemical source of urban organic emissions, Science 359 (2018) 760–764.

[36] https://www.tofwerk.com/industrial-indoor-air-quality-monitoring/.

[37] https://www.berkeleyanalytical.com/; https://www.pati-air.com/technical-data-sheets.

[38] J.Y. Li, R.M. Chen, W. Cui, X.A. Dong, H. Wang, K.H. Kim, Y.H. Chu, J.P. Sheng, Y. J. Sun, F. Dong, Synergistic photocatalytic decomposition of VOCs mixture: high efficiency, reaction mechanism, and long-term stability, ACS Catal. 10 (2020) 7230–7239.

[39] X.C. Jin, C. Li, C.B. Xu, D.W. Guan, A. Cheruvathur, Y. Wang, J. Xu, Dong Wei, H. W. Xiang, J.W. Niemantsverdriet, Y.W. Li, Q. Guo, Z.B. Ma, R. Su, X.M. Yang, Photocatalytic C-C bond cleavage in ethylene glycol on TiO_2: a molecular level picture and the effect of metal nanoparticles, J. Catal. 354 (2017) 37–45.

[40] H.L. Dou, D. Long, X. Rao, Y.P. Zhang, Y.M. Qin, F. Pan, K. Wu, Photocatalytic degradation kinetics of gaseous formaldehyde flow using TiO_2 nanowires, ACS Sustain. Chem. Eng. 7 (2019) 4456–4465.

[41] Y.T. Dai, P.J. Ren, Y.R. Li, D.D. Lv, Y.B. Shen, Y.W. Li, J.W. Niemantsverdriet, F. Besenbacher, H.W. Xiang, W.C. Hao, N. Lock, X.D. Wen, J.P. Lewis, R. Su, Solid base $Bi_{24}O_{31}Br_{10}(OH)_\sigma$ with active lattice oxygen for the efficient photo-oxidation of primary alcohols to aldehydes, Angew. Chem. Int. Ed. 58 (2019) 6265–6270.

[42] T. Sato, V.V. Plashnitsa, M. Utiyama, N. Miura, YSZ-based sensor using NiO sensing electrode for detection of volatile organic compounds in ppb level, J. Electrochem. Soc. 158 (2011) J175–J178.

[43] J. Michalowicz, W. Duda, Phenols – sources and toxicity, Pol. J. Environ. Stud. 16 (2007) 347–362.

[44] J. Devillers, Acute toxicity of cresols, xylenols, and trimethylphenols to *daphnia magna* straus 1820, Sci. Total Environ. 76 (1988) 79–83.

[45] R. Long, H. Huang, Y.P. Li, L. Song, Y.J. Xiong, Palladium-based nanomaterials: a platform to produce reactive oxygenspecies for catalyzing oxidation reactions, Adv. Mater. 27 (2015) 7025–7042.

[46] D.L. Marshall, M.L. Christian, G. Gryn'ova, M.L. Coote, P.J. Barkera, S.J. Blanksby, Oxidation of 4-substituted TEMPO derivatives reveals modifications at the 1- and 4-positions, Org. Biomol. Chem. 9 (2011) 4936–4947.

[47] S. Furukawa, M. Endo, T. Komatsu, Bifunctional catalytic system effective for oxidative dehydrogenation of 1-butene and n-butane using Pd-based intermetallic compounds, ACS Catal. 4 (2014) 3533–3542.

[48] G.R. Buettner, Spin trapping: ESR parameters of spin adducts, Free Rad. Biol. Med. 3 (1987) 259–303.

[49] D.A. Stoyanovsky, Z. Melnikov, A.I. Cederbaum, ESR and HPLC-EC analysis of the interaction of hydroxyl radical with DMSO: rapid reduction and quantification of POBN and PBN nitroxides, Anal. Chem. 71 (1999) 715–721.